Aminocarbyne Coupling Reactions at $M(Ph_2PCH_2CH_2PPh_2)_2$ (M = Mo or W) Sites. Detailed Mechanistic Studies on the Protonation of Co-ordinated Isocyanides and Coupling of Ligands in *trans*-$[M(CNR)_2(Ph_2PCH_2CH_2PPh_2)_2]$ (R = Bu^t or Me)†

Richard A. Henderson,*[a] Armando J. L. Pombeiro,*[b] Raymond L. Richards,[a] João J. R. Fraústo da Silva[b] and Yu Wang[b]

[a] *AFRC IPSR Nitrogen Fixation Laboratory, University of Sussex, Brighton BN1 9RQ, UK*

[b] *Centro de Quimica Estrutural, Instituto Superior Tecnico, Av. Rovisco Pais, 1096 Lisboa codex, Portugal*

The mechanism of protonation of *trans*-$[M(CNR)_2(dppe)_2]$ (M = Mo or W, R = Me or Bu^t, dppe = $Ph_2PCH_2CH_2PPh_2$) has been shown to involve the initial rapid protonation of an isocyanide ligand to form *trans*-$[M(CNHR)(CNR)(dppe)_2]^+$ which can then undergo rate-limiting intramolecular migration of the hydrogen to form $[MH(CNR)_2(dppe)_2]^+$. For *trans*-$[Mo(CNBu^t)_2(dppe)_2]$ an additional acid-catalysed pathway is observed involving the intermediate $[MoH(CNHBu^t)(CNBu^t)(dppe)_2]^{2+}$ which subsequently rapidly releases a proton from the aminocarbyne to produce the hydrido complex. The formation of the diaminoacetylene complex, *trans*-$[MoCl(\eta^2\text{-MeHNC}{\equiv}\text{CNHMe})(dppe)_2]^+$ occurs in three distinct steps. First is the rapid protonation of the isocyanide ligand to form *trans*-$[Mo(CNHMe)(CNMe)(dppe)_2]^+$, which at low concentrations of acid undergoes intramolecular hydrogen migration to produce the hydrido complex but at high acid concentrations rapidly forms *trans*-$[Mo(CNHMe)_2(dppe)_2]^{2+}$. It is this bis(aminocarbyne) species which in the second step is attacked by Cl^- and subsequently undergoes intramolecular *trans* to *cis* isomerisation followed by coupling of the aminocarbyne ligands to form the product, *trans*-$[MoCl(\eta^2\text{-MeHNC}{\equiv}\text{CNHMe})(dppe)_2]^+$.

Previous synthetic studies[1-3] have shown that protonation of *trans*-$[M(CNR)_2(dppe)_2]$ (M = Mo or W, dppe = $Ph_2PCH_2CH_2PPh_2$, R = alkyl group) with HA can result in the formation of the following types of complexes: *trans*-$[M(CNHR)(CNR)(dppe)_2]A$,[2] *trans*-$[M(CNHR)_2(dppe)_2]A_2$,[1] $[MH(CNR)_2(dppe)_2]A$,[2] $[MH(CNHR)(CNR)(dppe)_2]A_2$[2] and *trans*-$[MF(\eta^2\text{-MeHNC}{\equiv}\text{CNHMe})(dppe)_2]A$[1,3] (A = BF_4, Cl or ClO_4). The product isolated depends on the nature of the metal, the alkyl substituent, the solvent, the acid used and the time of the reaction. Herein we report the first kinetic studies on the protonation of isocyanide complexes. This study defines for the first time (*i*) the rates of protonation at the various sites (metal or isocyanide) and (*ii*) the factors which define the acid-catalysed coupling reaction to form $[MCl(\eta^2\text{-MeHNC}{\equiv}\text{CNHMe})(dppe)_2]^+$. This latter reaction has been the subject of much speculation mechanistically.[4,5] Previous mechanistic considerations[4,5] have stressed the importance of aminocarbyne intermediates and the possibility that the act of coupling is promoted by nucleophilic attack. In addition, the importance of steric factors and electronic influences of co-ligands (particularly of π-electron-releasing groups) in facilitating the coupling have been emphasised. However, prior to the work described herein, no kinetic study has identified the reactive species.

Our approach to understanding the protonation reactions of these isocyanide complexes was to study initially the relatively simple reaction of *trans*-$[M(CNBu^t)_2(dppe)_2]$ (M = Mo or W) with HCl to give $[MH(CNBu^t)_2(dppe)_2]^+$. With the characteristics of these simple reactions defined, the more complex protonation and coupling reactions of *trans*-$[Mo(CNMe)_2(dppe)_2]$ can be understood.

† *Supplementary data available* (No. SUP 57069, 3 pp.): Table of rate constants k_{obs}. See Instructions for Authors, *J. Chem. Soc., Dalton Trans.*, 1995, Issue 1, pp. xxv–xxx.

Results and Discussion

Protonation of trans-$[M(CNBu^t)_2(dppe)_2]$: *Formation of* $[MH(CNBu^t)_2(dppe)_2]^+$.—The reaction between *trans*-$[M(CNBu^t)_2(dppe)_2]$ (M = Mo or W) and an excess of anhydrous HCl in tetrahydrofuran (thf) gives stoichiometric production of $[MH(CNBu^t)_2(dppe)_2]^+$, equation (1).[6] When

$$\textit{trans}\text{-}[M(CNBu^t)_2(dppe)_2] + HCl \longrightarrow [MH(CNBu^t)_2(dppe)_2]Cl \quad (1)$$

monitored on a stopped-flow spectrophotometer, the reaction of HCl with the molybdenum complex occurs in two distinct phases: an initial rapid absorbance decrease which is complete within the dead-time of the stopped-flow apparatus (2 ms), followed by an exponential absorbance–time decay to yield the absorbance corresponding to the hydrido product.

The exponential absorbance–time decay demonstrates that the kinetics of the reaction exhibits a first-order dependence on the concentration of the complex. This dependence is confirmed by the observation that, at a constant acid concentration ([HCl] = 0.5 mmol dm^{-3}), the observed, pseudo-first-order rate constant (k_{obs}) is independent of the concentration of complex ([Mo(CNBu^t)$_2$(dppe)$_2$] = 0.05–0.2 mmol dm^{-3}; k_{obs} = 0.50 ± 0.03 s^{-1}).[7]

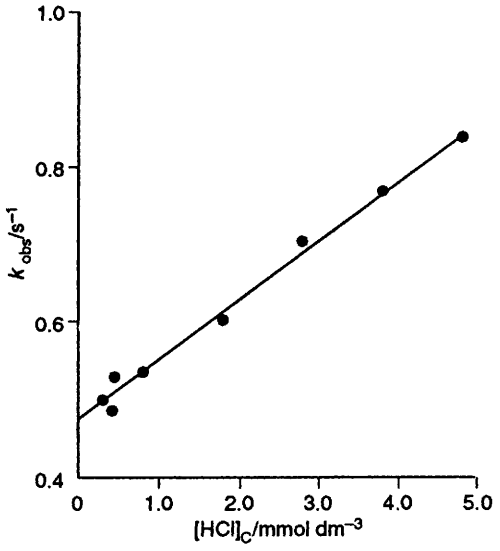

Fig. 1 Dependence of the corrected concentration of HCl, $[HCl]_c$, for the reaction between *trans*-$[Mo(CNBu^t)_2(dppe)_2]$ and HCl in thf at 25.0 °C. The concentration of HCl is corrected according to equation (3) to allow for the consumption of 1 mol equivalent of acid in the prior formation of *trans*-$[Mo(CNHBu^t)(CNBu^t)(dppe)_2]^+$. The line drawn is that defined by equation (2), using the values in the text

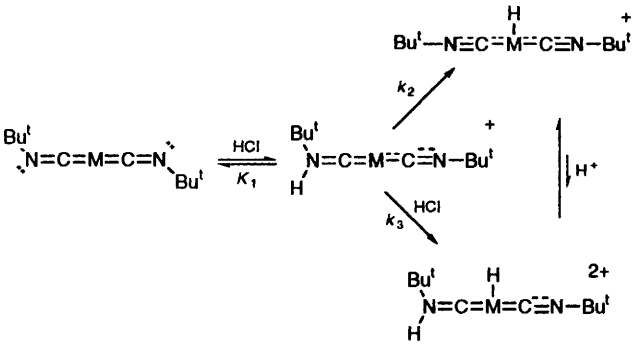

Scheme 1

The dependence of the rate of the reaction on the concentration of HCl is more complicated as shown by the data in Fig. 1. Both the kinetics and the absorbance–time behaviour are consistent with the mechanism shown in Scheme 1.

Initial rapid protonation of *trans*-$[Mo(CNBu^t)_2(dppe)_2]$ at an isocyanide ligand generates the aminocarbyne complex, *trans*-$[Mo(CNHBu^t)(CNBu^t)(dppe)_2]^+$. This step occurs within the dead-time of the stopped-flow apparatus and we can estimate a limit to the rate constant of this protonation, $k_1 \geqslant 1 \times 10^5$ dm^3 mol^{-1} s^{-1}, assuming a first-order dependence on the concentration of HCl. This value is consistent with other studies on the protonation of a wide variety of different ligands such as dinitrogen,[8] nitriles[9] and unsaturated hydrocarbons[10] bound to the electron-rich 'M(dppe)$_2$' core (M = Mo, W or Re). In all systems the initial site of protonation is the atom remote from the metal and it seems likely that these reactions occur at, or close to, the diffusion-controlled limit ($k_{diff} = 1 \times 10^{11}$ dm^3 mol^{-1} s^{-1}).

The proposal that the intermediate detected in this reaction is *trans*-$[Mo(CNHBu^t)(CNBu^t)(dppe)_2]^+$ is consistent with the observation[11] that the tungsten analogue, *trans*-$[W(CNHBu^t)(CNBu^t)(dppe)_2]^+$ has been isolated by performing the reaction in benzene from which this complex readily precipitates.

The subsequent exponential absorbance–time decay corresponds to the conversion of *trans*-$[Mo(CNHBu^t)(CNBu^t)(dppe)_2]^+$ to $[MoH(CNBu^t)_2(dppe)_2]^+$. The rate law for this process is given by equation (2) which describes two pathways

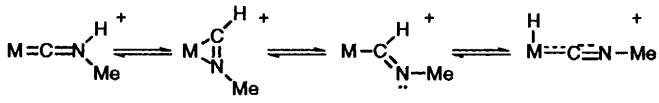

Fig. 2 Proposed mechanism for the intramolecular rearrangement of an aminocarbyne ligand to the corresponding hydrido, isocyanide species

$$-d[Mo(CNHBu^t)(CNBu^t)(dppe)_2^+]/dt = (k_2 + k_3[HCl]_c)[Mo(CNHBu^t)(CNBu^t)(dppe)_2^+] \quad (2)$$

by which this transformation is accomplished: an acid-independent and an acid-dependent route. The derivation of this rate law assumes that the rate-limiting steps are the intramolecular migration and the protonation of the metal in the acid-independent and acid-dependent pathways, respectively.

In analysing the true dependence on the concentration of HCl allowance must be made for the consumption of 1 mole equivalent of acid in the prior formation of *trans*-$[Mo(CNHBu^t)(CNBu^t)(dppe)_2]^+$, as shown in equation (3). In this

$$[HCl]_c = [HCl] - [Mo(CNBu^t)_2(dppe)_2] \quad (3)$$

equation (and in the remainder of this paper) $[HCl]_c$ is the corrected concentration of acid and [HCl] is the concentration of acid initially added to the reaction mixture. Having incorporated this correction the values $k_2 = (0.48 \pm 0.01)$ s^{-1} and $k_3 = (76.4 \pm 2.2)$ dm^3 mol^{-1} s^{-1} can be derived from the data in Fig. 1.

The details of the intramolecular pathway (k_2) are worthy of further comment. It seems likely that this rearrangement involves an initial formation of *trans*-$[Mo(\eta^2\text{-}CHNBu^t)(CNBu^t)(dppe)_2]^+$, from which the proton can move to the molybdenum with concomitant change in the ligation of the isocyanide ligand, as shown in Fig. 2.

The reaction of the tungsten analogue, *trans*-$[W(CNBu^t)_2(dppe)_2]$ with an excess of anhydrous HCl in thf shows similar behaviour to that of the molybdenum complex: an initial absorbance decrease complete within the dead-time of the apparatus followed by an exponential absorbance–time decay to yield the product, $[WH(CNBu^t)_2(dppe)_2]^+$. This behaviour is consistent with the mechanism shown in Scheme 1. Thus, we propose that the initial site of protonation is an isocyanide ligand to give *trans*-$[W(CNHBu^t)(CNBu^t)(dppe)_2]^+$ ($k_1 \geqslant 5 \times 10^5$ dm^3 mol^{-1} s^{-1}). The exponential absorbance–time trace associated with the conversion of *trans*-$[W(CNHBu^t)(CNBu^t)(dppe)_2]^+$ to $[WH(CNBu^t)_2(dppe)_2]^+$ is consistent with a first-order dependence on the concentration of the aminocarbyne complex. This is confirmed by studies in which the concentration of complex was varied ($[W(CNBu^t)_2(dppe)_2] = 0.019$–$0.3$ mmol dm^{-3}), at a constant acid concentration, [HCl] = 0.5 mmol dm^{-3}. Under these conditions the value of $k_{obs} = 1.21 \pm 0.08$ s^{-1} does not vary.

The rate of the reaction is independent of the concentration of acid, over the range [HCl] = 0.2–2.0 mmol dm^{-3}. Thus the rate law for the conversion of *trans*-$[W(CNHBu^t)(CNBu^t)(dppe)_2]^+$ to $[WH(CNBu^t)_2(dppe)_2]^+$ is given by equation (4).

$$-d[W(CNHBu^t)(CNBu^t)(dppe)_2^+]/dt = (1.25 \pm 0.06)[W(CNHBu^t)(CNBu^t)(dppe)_2^+] \quad (4)$$

This rate law demonstrates that *trans*-$[W(CNHBu^t)(CNBu^t)(dppe)_2]^+$ converts to $[WH(CNBu^t)_2(dppe)_2]^+$ exclusively by the intramolecular route ($k_2 = 1.25 \pm 0.06$ s^{-1}).

Protonation of trans-$[Mo(CNMe)_2(dppe)_2]$.—The reaction between *trans*-$[Mo(CNMe)_2(dppe)_2]$ and a *large excess* of

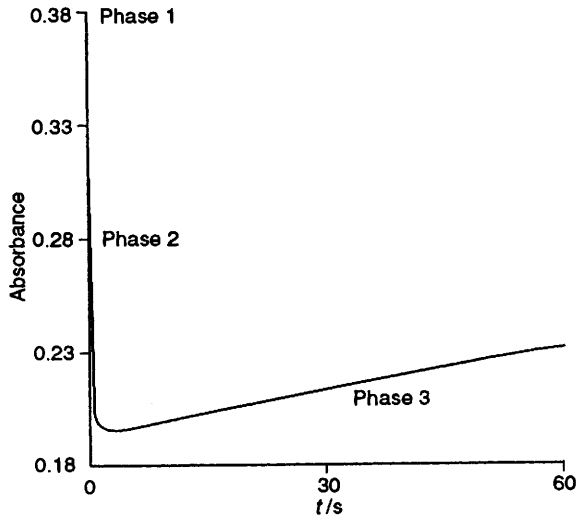

Fig. 3 Typical absorbance–time trace measured on the stopped-flow apparatus for the reaction between *trans*-$[Mo(CNMe)_2(dppe)_2]$ and HCl in thf at 25.0 °C, λ = 480 nm. This trace extends to 60 s, and shows phases 1, 2 and 3. Concentration of *trans*-$[Mo(CNMe)_2(dppe)_2]$ = 0.3 mmol dm^{-3}, concentration of HCl = 0.5 mmol dm^{-3}

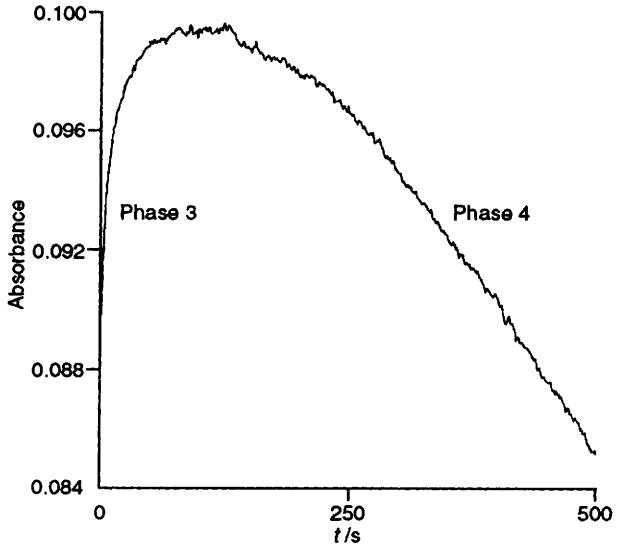

Fig. 4 Typical absorbance–time trace measured on the stopped-flow apparatus for the reaction between *trans*-$[Mo(CNMe)_2(dppe)_2]$ and HCl in thf at 25.0 °C, λ = 480 nm. This trace extends to 500 s, and shows phases 3 and 4 (not completed). Concentration of *trans*-$[Mo(CNMe)_2(dppe)_2]$ = 0.4 mmol dm^{-3}, concentration of HCl = 4.0 mmol dm^{-3}

anhydrous HCl in thf gives the diaminoacetylene complex, equation (5). When studied on a stopped-flow apparatus the

$$trans\text{-}[Mo(CNMe)_2(dppe)_2] + 3HCl \longrightarrow trans\text{-}[MoCl(\eta^2\text{-}MeHNC{\equiv}CNHMe)(dppe)_2][HCl_2] \quad (5)$$

reaction between *trans*-$[Mo(CNMe)_2(dppe)_2]$ and an excess of HCl is observed to occur in four well defined phases over the course of about 20 min. The entire reaction profile is shown in Fig. 3 (phases 1, 2 and 3) and Fig. 4 (phases 3 and 4).

The sequence of events is as follows. At all concentrations of HCl there is an initial rapid decrease in absorbance (phase 1) which is complete within the dead-time of the stopped-flow apparatus. At relatively low concentrations of HCl, this is followed by an exponential absorbance–time decay, which is complete within *ca.* 3 s (phase 2). At relatively high concentrations of HCl the absorbance subsequently increases over the next minute or so (phase 3), followed by the final absorbance decrease over about 20 min (phase 4).

Characterisation of the products. The relative magnitudes of phases 2 and 3 vary with the concentration of HCl. Phase 2 is associated with the largest absorbance change at low acid concentrations, but disappears completely at higher acid concentrations, when phase 3 becomes noticeable for the first time. This observation indicates that different products are formed at different concentrations of HCl.

Surprisingly, we observe that over only a five-fold change in HCl concentration the product changes completely. When $[HCl]/[Mo(CNMe)_2(dppe)_2] = 2.0$ the isolated product ($\geqslant$80%) is the hydrido species, $[MoH(CNMe)_2(dppe)_2]Cl$.[6] However, when $[HCl]/[Mo(CNMe)_2(dppe)_2] = 10.0$ the product isolated within *ca.* 1 min is predominantly *trans*-$[Mo(CNHMe)_2(dppe)_2]Cl_2$.[1] The products were characterised by ^1H, $^{31}P\text{-}\{^1H\}$ and ^{13}C NMR spectroscopy and IR spectroscopy.

Initial stages in the reaction: formation of aminocarbynes and hydrides. It is clear that phases 1 and 2 of the reaction between *trans*-$[Mo(CNMe)_2(dppe)_2]$ and HCl show great similarity to the behaviour of *trans*-$[M(CNBu^t)_2(dppe)_2]$ with HCl described in the earlier section, and rationalised by the mechanism shown in Scheme 1. Thus we propose that the initial absorbance decrease (phase 1 shown in Fig. 3) is due to the rapid ($k_1 \geqslant 1 \times 10^6$ dm^3 mol^{-1} s^{-1}) protonation of a methyl isocyanide ligand to form *trans*-$[Mo(CNHMe)(CNMe)(dppe)_2]^+$. The subsequent absorbance–time decay (phase 2) corresponds to the conversion of this aminocarbyne species to the hydride complex, $[MoH(CNMe)_2(dppe)_2]^+$. This hydrido species is the product isolated at relatively low acid concentrations. Further evidence that $[MoH(CNMe)_2(dppe)_2]^+$ is the product at the end of phase 2 comes from spectrophotometric studies. The molar absorption coefficient observed at the end of phase 2 (ε = 450 ± 10 dm^3 mol^{-1} s^{-1}, λ = 480 nm) was measured using the stopped-flow apparatus and is identical to that observed with an authentic sample of $[MoH(CNMe)_2(dppe)_2]^+$.

The exponential absorbance–time trace observed for the conversion of *trans*-$[Mo(CNHMe)(CNMe)(dppe)_2]^+$ to $[MoH(CNMe)_2(dppe)_2]^+$ is consistent with the rate of the reaction exhibiting a first-order dependence on the concentration of *trans*-$[Mo(CNHMe)(CNMe)(dppe)_2]^+$. Over the rather limited concentration range of HCl for which phase 2 is observed ($[HCl]_c$ = 0.2–0.35 mmol dm^{-3}), the rate of the reaction is independent of the concentration of HCl. The experimental rate law is that shown in equation (6). This rate

$$d[MoH(CNMe)_2(dppe)_2{}^+]/dt = 8.2[Mo(CNHMe)(CNMe)(dppe)_2{}^+] \quad (6)$$

law is consistent with an intramolecular pathway for hydrogen migration from isocyanide ligand to metal (k_2 = 8.2 s^{-1}) as shown in Scheme 2, and established above for the *tert*-butyl isocyanide analogues.

There is a further point concerning the initial phases in the protonation of *trans*-$[Mo(CNMe)_2(dppe)_2]$ which deserves clarification before we proceed. The initial absorbance jump (phase 1) is significant even in the presence of stoichiometric amounts of acid, $[HCl]/[Mo(CNMe)_2(dppe)_2] = 2.0$. In addition, the magnitude of this absorbance jump increases with the concentration of HCl. These two effects are due to protonation of *trans*-$[Mo(CNMe)_2(dppe)_2]$ to form an equilibrium mixture of *trans*-$[Mo(CNHMe)(CNMe)(dppe)_2]^+$ and *trans*-$[Mo(CNHMe)_2(dppe)_2]^{2+}$. The relative proportions of the two cations will depend on the concentration of HCl, the dication predominating at the higher acid concentrations. These changes

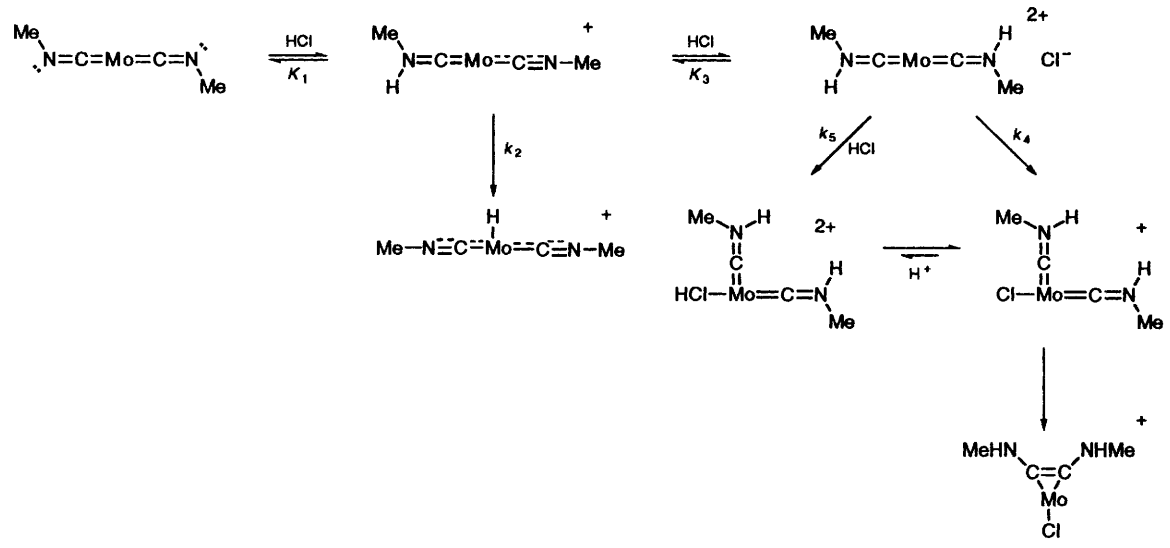

Scheme 2

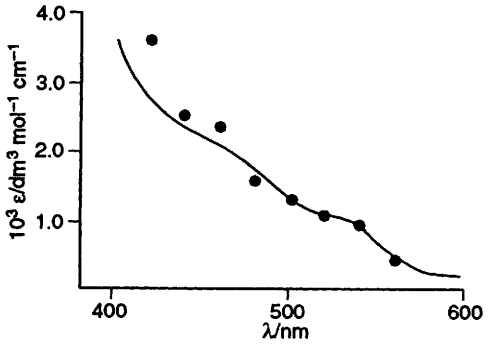

Fig. 5 Visible absorption spectrum of *trans*-[MoCl(η^2-MeHNC≡CNHMe)(dppe)$_2$]$^+$. Solid line is that measured for isolated *trans*-[MoCl(η^2-MeHNC≡CNHMe)(dppe)$_2$]Cl. The points (●) correspond to the spectrum of the species observed, at the end of phase 3, measured on the stopped-flow apparatus

in the concentrations of *trans*-[Mo(CNHMe)(CNMe)(dppe)$_2$]$^+$ and *trans*-[Mo(CNHMe)$_2$(dppe)$_2$]$^{2+}$ as the concentration of acid is varied have two important repercussions. First, the actual change in the free acid concentration, $[HCl]_c$ decreases and, secondly, the absorbance at the end of phase 1 decreases, since progressively more *trans*-[Mo(CNHMe)$_2$(dppe)$_2$]$^{2+}$ is generated. Consequently the absorbance change associated with the hydride-forming pathway (phase 2) becomes very small and ultimately undetectable, so that at relatively high concentrations of acid only phase 3 is observed. However, we assume that [MoH(CNMe)$_2$(dppe)$_2$]$^+$ is still being formed, but the absorbance change associated with the conversion of *trans*-[Mo(CNHMe)(CNMe)(dppe)$_2$]$^+$ to [MoH(CNMe)$_2$(dppe)$_2$]$^+$, in the presence of a significant amount of *trans*-[Mo(CNHMe)$_2$(dppe)$_2$]$^{2+}$, is too small to be detected.

Studies on the isolated complex, *trans*-[Mo(CNHMe)$_2$(dppe)$_2$][ClO$_4$]$_2$, show that this species is not capable of forming [MoH(CNMe)$_2$(dppe)$_2$]$^+$ on the time-scale associated with these stopped-flow experiments. Thus, at high acid concentrations we predict that the rate of formation of [MoH(CNMe)$_2$(dppe)$_2$]$^+$, from *trans*-[Mo(CNHMe)(CNMe)(dppe)$_2$]$^+$ is inhibited by HCl. This is a consequence of the unreactive *trans*-[Mo(CNHMe)$_2$(dppe)$_2$]$^{2+}$ being formed. Assuming that the protonation equilibrium between *trans*-[Mo(CNHMe)(CNMe)(dppe)$_2$]$^+$ and *trans*-[Mo(CNHMe)$_2$(dppe)$_2$]$^{2+}$ is established rapidly, compared to k_2, then the dependence of k_{obs} for the formation of [MoH(CNMe)$_2$(dppe)$_2$]$^+$ on the concentration of HCl is given by equation (7).

$$k_{obs} = k_2/(1 + K_3[HCl]) \quad (7)$$

Unfortunately, the narrow concentration range of HCl over which phase 2 is amenable to study means that this prediction cannot be tested, but as we will see in a later section this rate law predicts the product distribution at various acid concentrations.

The coupling step. Phase 3 of the reaction (Fig. 4) corresponds to the formation of *trans*-[MoCl(η^2-MeHNC≡CNHMe)(dppe)$_2$]$^+$ from the equilibrium mixture of *trans*-[Mo(CNHMe)(CNMe)(dppe)$_2$]$^+$ and *trans*-[Mo(CNHMe)$_2$(dppe)$_2$]$^{2+}$. As alluded to above, this coupling reaction is in competition with the formation of [MoH(CNMe)$_2$(dppe)$_2$]$^+$, and it must be emphasised that the hydrido complex is not capable of being transformed into the diaminoacetylene species. Indeed, the reaction of [MoH(CNMe)$_2$(dppe)$_2$]$^+$ with further acid results only in the relatively slow formation of [MoH(CNHMe)(CNMe)(dppe)$_2$]$^{2+}$.

The product at the end of phase 3 was identified as *trans*-[MoCl(η^2-MeHNC≡CNHMe)(dppe)$_2$]$^+$, not only by isolation and full spectroscopic characterisation[1] but also by measuring the visible absorption spectrum of the reaction solution on the stopped-flow apparatus at the end of phase 3 as shown in Fig. 5. This spectrum is essentially identical to that of an authentic sample of isolated *trans*-[MoCl(η^2-MeHNC≡CNHMe)(dppe)$_2$]Cl. It is only at low wavelengths that there is some difference between the two spectra. This slight difference is most probably due to a contribution to the total absorbance by the excess of HCl present in the reaction solution.

The exponential absorbance–time trace associated with phase 3 indicates a first-order dependence on the concentration of *trans*-[Mo(CNHMe)$_2$(dppe)$_2$]$^{2+}$. The dependence on the concentration of HCl is shown in Fig. 6. Thus the rate law for the formation of [MoCl(η^2-MeHNC≡CNHMe)(dppe)$_2$]$^+$ from *trans*-[Mo(CNHMe)$_2$(dppe)$_2$]$^{2+}$ is given by equation (8).

$$d[MoCl(\eta^2\text{-MeHNC}{\equiv}CNHMe)(dppe)_2{}^+]/dt = \{(1.1 \pm 0.1) \times 10^{-2} + (32.3 \pm 0.9)[HCl]_c\} \times [Mo(CNHMe)_2(dppe)_2{}^{2+}] \quad (8)$$

In both Fig. 6 and equation (8) the concentration of acid has been corrected according to equation (9) to allow

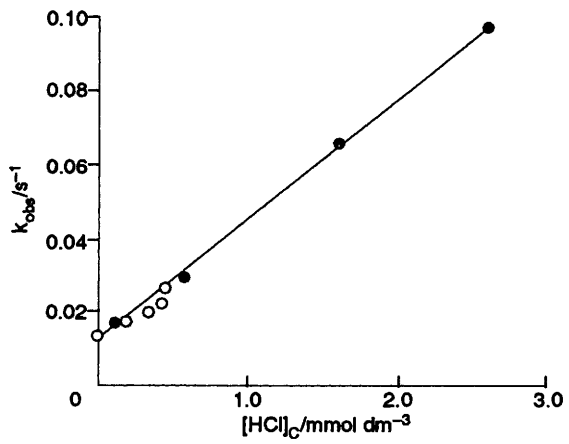

Fig. 6 The dependence of the corrected concentration of HCl, $[HCl]_c$, on k_{obs} for the conversion of *trans*-$[Mo(CNHMe)_2(dppe)_2]^{2+}$ to *trans*-$[MoCl(\eta^2\text{-MeHNC}{\equiv}CNHMe)(dppe)_2]^+$, in thf at 25.0 °C (phase 3). The concentration of HCl is corrected, using equation (9), to allow for the consumption of 2 mol equivalents of HCl in phases 1 and 2 whilst forming *trans*-$[Mo(CNHMe)_2(dppe)_2]^{2+}$. Data points correspond to: $[Mo(CNMe)_2(dppe)_2]$ = 0.019–0.30 mmol dm^{-3}, [HCl] = 0.5 mmol dm^{-3} (○); $[Mo(CNMe)_2(dppe)_2]$ = 0.20 mmol dm^{-3}, [HCl] = 0.50–3.0 mmol dm^{-3} (●). The line drawn is that defined by equation (8)

for the 2 mol equivalents of HCl consumed in phases 1 and 2.

$$[HCl]_c = [HCl] - 2[Mo(CNMe)_2(dppe)_2] \quad (9)$$

Phase 3 corresponds to the overall reaction shown in equation (10). This transformation must involve at least three

$$trans\text{-}[Mo(CNHMe)_2(dppe)_2]^{2+} + Cl^- \longrightarrow trans\text{-}[MoCl(\eta^2\text{-MeHNC}{\equiv}CNHMe)(dppe)_2]^+ \quad (10)$$

elementary reactions: an isomerisation step (to bring the aminocarbyne ligands adjacent to one another); the coupling of these ligands and the addition of chloride ion.

The two-term rate law shown in equation (8) indicates that there are two pathways by which *trans*-$[Mo(CNHMe)_2(dppe)_2]^{2+}$ is converted to *trans*-$[MoCl(\eta^2\text{-MeHNC}{\equiv}CNHMe)(dppe)_2]^+$. Clearly the coupling of the ligands cannot occur until after the *cis* to *trans* isomerisation step, but in principle ion attack could occur before or after the coupling reaction. The simplicity of the rate law for phase 3 means that on the basis of the kinetics alone we cannot distinguish between rate-limiting isomerisation or rate-limiting chloride ion attack. However, studies[1] on isolated *trans*-$[Mo(CNHMe)_2(dppe)_2][ClO_4]_2$ show that no *cis* to *trans* isomerisation processes occur and hence we conclude that the kinetics is associated with rate-limiting nucleophilic attack by chloride ion as shown in Scheme 2. The acid-independent term corresponds to the attack of chloride ion at the metal [$k_4 = (1.1 \pm 0.9) \times 10^{-2}$ s^{-1}]. Since thf is a solvent of low relative permittivity[12] there is extensive ion-pairing between chloride ion and *trans*-$[Mo(CNHMe)_2(dppe)_2]^{2+}$. Consequently the attack by chloride on the complex is from within this ion-pair and is thus a first-order process. If this interpretation is correct then the addition of a chloride salt, $[NR_4]Cl$, would not affect the kinetics of this pathway. However, the limited solubility of chloride salts in thf meant we could not rigorously test this proposal.

The relatively high positive charge of $[Mo(CNHMe)_2(dppe)_2]^{2+}$ makes it unlikely that this species is susceptible to further protonation. It seems more likely that the acid-dependent term in equation (8) corresponds to the attack by the chlorine atom, in HCl, at *trans*-$[Mo(CNHMe)_2(dppe)_2]^{2+}$ [$k_5 = (32.3 \pm 0.9)$ dm^3 mol^{-1} s^{-1}]. This is followed by rapid loss of a proton. In thf, HCl is only poorly dissociated, thus limiting the concentration of free chloride ion. Hence, in a reaction relying on attack by a nucleophile it seems likely that the system must find alternative sources of the nucleophile, such as the undissociated acid, HCl.

Since *trans*-$[Mo(CNHMe)_2(dppe)_2]^{2+}$ requires no further protons to form the diaminoacetylene complex, the acid dependence for this step observed in equation (8) must be catalytic. This is confirmed by studies at very low concentrations of HCl. Under conditions where $2[HCl] \approx [Mo(CNMe)_2(dppe)_2]$ the absorbance–time traces are still exponential. In addition, if the concentration of acid is kept constant but the concentration of complex is varied the rate of the reaction varies. Studies with [HCl] = 0.5 mmol dm^{-3}, $[Mo(CNMe)_2(dppe)_2]$ = 0.019–0.30 mmol dm^{-3} are shown in Fig. 6. Even under these conditions the variation in k_{obs} with $[HCl]_c$ is defined by equation (8). This is consistent with our interpretation of the processes occurring in phases 1 and 2. In particular, it confirms our proposal that the species formed at the end of phase 1, at high acid concentrations, is *trans*-$[Mo(CNHMe)_2(dppe)_2]^{2+}$ and it is this species which is the essential intermediate that goes on to form *trans*-$[MoCl(\eta^2\text{-MeHNC}{\equiv}CNHMe)(dppe)_2]^+$. Previous mechanistic proposals[4,5] have implicated bis(aminocarbyne) complexes as intermediates in this type of reaction, and in this study our full quantitative analysis has demonstrated unambiguously the crucial role of such species.

The final phase (phase 4) of the reaction between *trans*-$[Mo(CNMe)_2(dppe)_2]$ and an excess of HCl corresponds to the further protonation of *trans*-$[MoCl(\eta^2\text{-MeHNC}{\equiv}CNHMe)(dppe)_2]^+$. This protonation has been observed before,[2] but it is still not entirely clear where it occurs. This final phase was so slow we were unable to study it to completion without traces of dioxygen seeping into the apparatus and interfering with the reaction.

The product distribution. As alluded to earlier, a notable feature of the product distribution is the narrow range of HCl concentration over which the product changes from $[MoH(CNMe)_2(dppe)_2]^+$ to *trans*-$[MoCl(\eta^2\text{-MeHNC}{\equiv}CNHMe)(dppe)_2]^+$. We can predict this change in the product approximately from consideration of the kinetics of formation of the two products. However, the experimental difficulties of rigorously quantifying the product composition, for any given acid concentration, mean that we can only demonstrate general trends in this analysis.

The rate law for the formation of $[MoH(CNMe)_2(dppe)_2]^+$ from *trans*-$[Mo(CNHMe)(CNMe)(dppe)_2]^+$, in the presence of a large excess of HCl, is given by equation (7); this rate law is rewritten in equation (11) using the rate and equilibrium

$$d[MoH(CNMe)_2(dppe)_2{}^+]/dt = k_2[Mo(CNHMe)(CNMe)(dppe)_2{}^+]/(1 + K_3[HCl]) \quad (11)$$

constants from Scheme 2.

The rate law for the formation of *trans*-$[MoCl(\eta^2\text{-MeHNC}{\equiv}CNHMe)(dppe)_2]^+$ is given in equation (8), but this is the rate expression starting from *trans*-$[Mo(CNHMe)_2(dppe)_2]^{2+}$. We can rewrite this rate law but now describing the kinetics of formation of the diaminoacetylene complex from *trans*-$[Mo(CNHMe)(CNMe)(dppe)_2]^+$ as shown in equation (12).

$$d[MoCl(\eta^2\text{-MeHNC}{\equiv}CNHMe)(dppe)_2{}^+]/dt = (k_4 + k_5[HCl])K_3[HCl][Mo(CNHMe)(CNMe)(dppe)_2{}^+]/(1 + K_3[HCl]) \quad (12)$$

Equations (11) and (12) describe the rate of formation of the hydrido and diaminoacetylene products, respectively from the common precursor, *trans*-$[Mo(CNHMe)(CNMe)(dppe)_2]^+$.

$$\frac{[MoH(CNMe)_2(dppe)_2^+]}{[MoH(CNMe)_2(dppe)_2^+] + [MoCl(\eta^2\text{-}MeHNC{\equiv}CNHMe)(dppe)_2^+]} = \frac{k_2}{k_2 + (k_4 + k_5[HCl])K_3[HCl]} \quad (13)$$

$$\frac{[MoCl(\eta^2\text{-}MeHNC{\equiv}CNHMe)(dppe)_2^+]}{[MoH(CNMe)_2(dppe)_2]^+ + [MoCl(\eta^2\text{-}MeHNC{\equiv}CNHMe)(dppe)_2^+]} = \frac{(k_4 + k_5[HCl])K_3[HCl]}{k_2 + (k_4 + k_5[HCl])K_3[HCl]} \quad (14)$$

We can now derive the expressions for the proportion of product which is the hydride complex [equation (13)], and the proportion of product which is the diaminoacetylene complex [equation (14)].

The elementary rate constants, k_2, k_4 and k_5 are known from our analysis of the kinetics. In addition, since phase 2 is not observed when [HCl] $\geqslant$ 0.5 mmol dm^{-3}, $K_3 \geqslant 1 \times 10^3$ dm^3 mol^{-1}. Using these values, the product distribution over the range [HCl] = 0–100 mmol dm^{-3} is that shown in Fig. 7. Thus when *trans*-[Mo(CNMe)$_2$(dppe)$_2$] = 2.0 mmol dm^{-3}, for [HCl]/[Mo] = 2.0, *ca.* 94% of the product is [MoH(CNMe)$_2$(dppe)$_2$]$^+$ whereas just increasing the acid concentration by a factor of 10, [HCl]/[Mo] = 20.0, the hydride now represents < 40% of the total product, and the dominant product is *trans*-[MoCl(η^2-MeHNC≡CNHMe)(dppe)$_2$]$^+$.

Conclusion

We have shown that the protonation of the complexes *trans*-[M(CNR)$_2$(dppe)$_2$] (R = Me or Bu^t, M = Mo or W) occurs preferentially at the isocyanide ligand to give *trans*-[M(CNHR)(CNR)(dppe)$_2$]$^+$ which rearranges to [MH(CNR)$_2$(dppe)$_2$]$^+$ by an intramolecular migration, or an acid-catalysed pathway. For *trans*-[Mo(CNHMe)(CNMe)(dppe)$_2$]$^+$ further rapid protonation of the isocyanide ligand at high concentrations of acid generates *trans*-[Mo(CNHMe)$_2$(dppe)$_2$]$^{2+}$ which reacts with sources of chloride to give *trans*-[MoCl(η^2-MeHNC≡CNHMe)(dppe)$_2$]$^+$. All these complexes have been isolated and structurally characterised.[1-3,6,11]

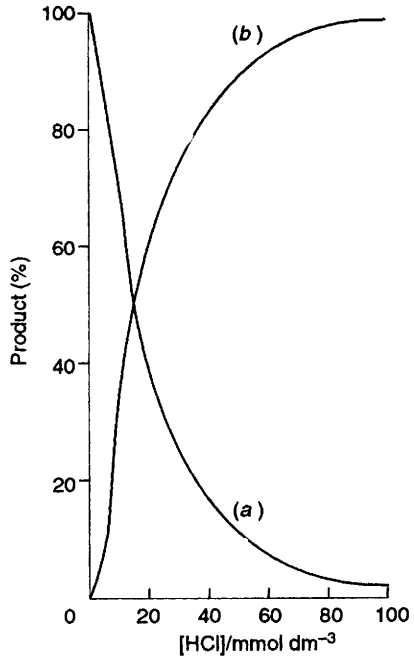

Fig. 7 Predicted product distribution for the reaction between *trans*-[Mo(CNMe)$_2$(dppe)$_2$] and HCl in thf at 25.0 °C. The curves show the proportion of the total product which is (*a*) [MoH(CNMe)$_2$(dppe)$_2$]$^+$ (predicted 100% at low [HCl]) or (*b*) *trans*-[MoCl(η^2-MeHNC≡CNHMe)(dppe)$_2$]$^+$ (predicted 100% at high [HCl]). The curves drawn are those defined by equations (13) and (14), respectively, using the values in the text

Experimental

All manipulations were routinely performed under an atmosphere of dinitrogen using Schlenk or syringe techniques as appropriate. The thf solvent was freshly distilled immediately prior to use. All complexes described in this paper were prepared and characterised by the methods described in the previous paper.[1]

Preparation of HCl *Solutions*.—Standard solutions of anhydrous HCl were prepared in thf under dinitrogen by mixing equimolar amounts of MeOH and SiMe$_3$Cl. Diluted solutions of acid were prepared from this stock solution. All solutions were used within 1 h to minimise any complications from the acid-catalysed decomposition of thf. All solutions were transferred to the stopped-flow apparatus using gas-tight all-glass syringes.

Kinetics Studies.—All kinetics were studied at 25.0 °C on a Canterbury SF-40 stopped-flow spectrophotometer with a SU-40 spectrophotometer unit from Hi-Tech Scientific.

The kinetics associated with the reactions of the isocyanide complexes was monitored at the wavelengths defined in the text. The rate constants were independent of the wavelength in the range 350–500 nm. The wavelength chosen for each complex was that giving the maximum absorbance change and the maximum signal-to-noise value.

For *trans*-[M(CNBu^t)$_2$(dppe)$_2$] (M = Mo or W), the absorbance–time curves were a single exponential. The absorbance–time traces were exponential for at least three half-lives. For *trans*-[Mo(CNMe)$_2$(dppe)$_2$] the reaction occurs in four distinct phases as shown in Figs. 3 and 4; each phase occurs by a well defined exponential absorbance–time trace.

For all systems and all phases the rate constants together with the initial and final absorbances were computed using the Rapid Kinetics Software Suite (version 1.0) program on a City Desk 386-SX computer interfaced to the stopped-flow spectrophotometer. The absorbance–time traces were exponential for at least three half-lives. The values of the rate constants reported in Figs. 1 and 6, and in SUP 57069 are the average of at least three independent experiments, all of which agree to within 5%.

Most of the reactions were studied under pseudo-first-order conditions, [HCl]/[M(CNR)$_2$(dppe)$_2$] $\geqslant$ 10. In these studies the dependence on the concentration of HCl was determined by systematically varying the concentration of the acid. A graph of k_{obs} (pseudo-first-order rate constant) against the concentration of HCl was then plotted and the data fitted using a least-squares analysis to derive the rate law. The reactions of *trans*-[Mo(CNMe)$_2$(dppe)$_2$] were studied in the range [HCl]/[Mo(CNMe)$_2$(dppe)$_2$] = 1.7–26.3. Under these conditions all phases of the multiphase absorbance–time traces were exponentials for at least three half-lives. In analysing the acid dependence of the later phases of these traces the concentration of acid was corrected (see Results and Discussion section) to allow for any acid consumed in the earlier phases.

Acknowledgements

This work has been partially supported by JNICT as well as the British Council/JNICT Protocol. We also acknowledge the Oriente Foundation for a fellowship (to Y. W.).

References

1 Y. Wang, J. J. R. Fraústo da Silva, A. J. L. Pombeiro, M. A. Pellinghelli, A. Tiripicchio, R. A. Henderson and R. L. Richards, preceding paper.
2 A. J. L. Pombeiro and R. L. Richards, *Transition Met. Chem.*, 1980, **5**, 55 and refs. therein.
3 J. J. R. F. da Silva, M. A. Pellinghelli, A. J. L. Pombeiro, R. L. Richards, A. Tiripicchio and Y. Wang, *J. Organomet. Chem.*, 1993, **454**, C8.
4 A. C. Filippou, *Polyhedron*, 1990, **9**, 727 and refs. therein; A. C. Filippou, W. Grünleitner, C. Völkl and P. Kiprof, *Angew. Chem., Int. Ed. Engl.*, 1991, **30**, 1167; A. Mayr, in *Transition Metal Carbyne Complexes*, ed. F. R. Kreissl, NATO ASI Series C, vol. 392, Kluwer Academic, Dordrecht, 1993, p. 219.
5 S. Warner and S. J. Lippard, *Organometallics*, 1989, **8**, 228 and refs. therein.
6 J. Chatt, A. J. L. Pombeiro and R. L. Richards, *J. Chem. Soc., Dalton Trans.*, 1979, 1585.
7 R. G. Wilkins, *Kinetics and Mechanism of Reactions of Transition Metal Complexes*, VCH, Weinheim, 1991, p. 5.
8 D. J. Evans, R. A. Henderson and B. E. Smith, *Bioinorganic Catalysis*, ed. J. Reedijk, Marcel-Dekker, New York, 1993, p. 89 and refs. therein.
9 J. J. R. Fraústo da Silva, M. F. C. Guedes da Silva, R. A. Henderson, A. J. L. Pombeiro and R. L. Richards, *J. Organomet. Chem.*, 1993, **461**, 141.
10 K. E. Oglieve and R. A. Henderson, *J. Chem. Soc., Chem. Commun.*, 1993, 474 and refs. therein.
11 J. Chatt, A. J. L. Pombeiro and R. L. Richards, *J. Chem. Soc., Dalton Trans.*, 1980, 492.
12 R. W. Alder, R. Baker and J. M. Brown, *Mechanism in Organic Chemistry*, Wiley Interscience, London, 1971, p. 41.

Received 15*th August* 1994; *Paper* 4/04979I